PET of Somatostatin Receptor–Positive Tumors Using ^{64}Cu- and ^{68}Ga-Somatostatin Antagonists: The Chelate Makes the Difference

Melpomeni Fani[1,2], Luigi Del Pozzo[1,2], Keelara Abiraj[1], Rosalba Mansi[1,2], Maria Luisa Tamma[1], Renzo Cescato[3], Beatrice Waser[3], Wolfgang A. Weber[2], Jean Claude Reubi[3], and Helmut R. Maecke[1,2]

[1]Division of Radiological Chemistry, University Hospital Basel, Basel, Switzerland; [2]Department of Nuclear Medicine, University Hospital Freiburg, Freiburg, Germany; and [3]Division of Cell Biology and Experimental Cancer Research, Institute of Pathology, University of Bern, Bern, Switzerland

Somatostatin-based radiolabeled peptides have been successfully introduced into the clinic for targeted imaging and radionuclide therapy of somatostatin receptor (sst)–positive tumors, especially of subtype 2 (sst2). The clinically used peptides are exclusively agonists. Recently, we showed that radiolabeled antagonists may be preferable to agonists because they showed better pharmacokinetics, including higher tumor uptake. Factors determining the performance of radioantagonists have only scarcely been studied. Here, we report on the development and evaluation of four ^{64}Cu or ^{68}Ga radioantagonists for PET of sst2-positive tumors. **Methods:** The novel antagonist *p*-Cl-Phe-cyclo(D-Cys-Tyr-D-4-amino-Phe(carbamoyl)-Lys-Thr-Cys)D-Tyr-NH_2 (LM3) was coupled to 3 macrocyclic chelators, namely 4,11-bis(carboxymethyl)-1,4,8,11-tetraazabicyclo[6.6.2]hexadecane (CB-TE2A), 1,4,7-triazacyclononane,1-glutaric acid-4,7-acetic acid (NODAGA), and DOTA. $^{64/nat}$Cu- and $^{68/nat}$Ga-NODAGA-LM3 were prepared at room temperature, and $^{64/nat}$Cu-CB-TE2A-LM3 and $^{68/nat}$Ga-DOTA-LM3 were prepared at 95°C. Binding affinity and antagonistic properties were determined with receptor autoradiography and immunofluorescence microscopy using human embryonic kidney (HEK)-sst2 cells. In vitro internalization and dissociation was evaluated using the same cell line. Biodistribution and small-animal PET studies were performed with HEK-sst2 xenografts. **Results:** All metallopeptides demonstrated antagonistic properties. The affinities depend on chelator and radiometal and vary about 10-fold; $^{68/nat}$Ga-NODAGA-LM3 has the lowest half maximal inhibitory concentration (1.3 ± 0.3 nmol/L). The biodistribution studies show impressive tumor uptake at 1 h after injection, particularly of ^{64}Cu- and ^{68}Ga-NODAGA-LM3 (~40 percentage injected dose per gram of tissue [%ID/g]), which were proven to be specific. Background clearance was fast and the tumor washout relatively slow for ^{64}Cu-NODAGA-LM3 (~15 %ID/g, 24 h after injection) and almost negligible for ^{64}Cu-CB-TE2A-LM3 (26.9 ± 3.3 %ID/g and 21.6 ± 2.1 %ID/g, 4 and 24 h after injection, respectively). Tumor–to–normal-tissue ratios were significantly higher for ^{64}Cu-NODAGA-LM3 than for ^{64}Cu-CB-TE2A-LM3 (tumor-to-kidney, 12.8 ± 3.6 and 1.7 ± 0.3, respectively; tumor-to-muscle, 1,342 ± 115 and 75.2 ± 8.5, respectively, at 24 h, $P < 0.001$). Small-animal PET shows clear tumor localization and high image contrast, especially for ^{64}Cu- and ^{68}Ga-NODAGA-LM3. **Conclusion:** This article demonstrates the strong dependence of the affinity and pharmacokinetics of the somatostatin-based radioantagonists on the chelator and radiometal. ^{64}Cu- and ^{68}Ga-NODAGA-LM3 and ^{64}Cu-CB-TE2A-LM3 are promising candidates for clinical translation because of their favorable pharmacokinetics and the high image contrast on PET scans.

Key Words: somatostatin antagonists; ^{64}Cu PET/CT; ^{68}Ga PET/CT; receptor targeting

J Nucl Med 2011; 52:1110–1118
DOI: 10.2967/jnumed.111.087999

The biologic actions of the neurohormone somatostatin are mediated by 5 receptor subtypes (somatostatin receptor subtype 1–5 [sst1–sst5]), all of which were found to be overexpressed to some degree on neuroendocrine tumors in humans, with sst2 being the most important one (*1*). Targeting of sst-positive tumors with radiolabeled peptides is of high interest for tumor localization, staging, therapy follow-up, and targeted radionuclide therapy (*2*). Several imaging probes based on γ- and positron emitters were developed. In European and Asian countries, thousands of patients were studied with ^{68}Ga-DOTATOC, ^{68}Ga-DOTATATE, and ^{68}Ga-DOTANOC (*3–5*). The same conjugates are being used in targeted radionuclide therapy with the ^{90}Y or ^{177}Lu labels (*6,7*).

These peptides are potent agonists, which are considered preferable over antagonists because agonists become internalized on binding to the receptor, demonstrating an important mechanism for accumulation and retention in tumor cells. We have recently shown that sst2 and sst3 selective antagonists have higher tumor uptake in mice bearing corresponding tumors and have generally improved pharmacokinetics, including lower kidney retention and faster clearance from the body (*8*). The higher tumor uptake was explained by the

Received Jan. 14, 2011; revision accepted Mar. 18, 2011.
For correspondence or reprints contact: Helmut R. Maecke, Department of Nuclear Medicine, University Hospital Freiburg, Hugstetterstrasse 55, D-79106 Freiburg, Germany.
E-mail: helmut.maecke@uniklinik-freiburg.de

higher number of binding sites recognized by antagonists, compared with agonists. Wadas et al., in the frequently used rat pancreatic cell line AR42J, compared the antagonist *p*-NO_2-Phe-cyclo(D-Cys-Tyr-D-Trp-Lys-Thr-Cys)D-Tyr-NH_2 (sst2-ANT) with the powerful agonist TATE, both conjugated to 4,11-bis(carboxymethyl)-1,4,8,11-tetraazabicyclo [6.6.2]hexadecane (CB-TE2A) and labeled with ^{64}Cu (*9*). Interestingly, they did not find the superiority of the antagonist, despite the fact that a 14-fold-higher number of binding sites for the antagonist was found, a result similar to what we found with our transfected human embryonic kidney (HEK)-sst2 cell line for ^{111}In-DOTA-sst2-ANT, compared with TATE, consequently a distinctly higher tumor uptake in vivo (*8*). These data indicate that the in vitro and in vivo properties of radiolabeled G-protein–coupled receptor antagonists are not yet understood well and need further studies.

We developed PET radiopharmaceuticals based on ^{68}Ga and ^{64}Cu. ^{68}Ga (half-life, 67.71 min; average positron energy [$\bar{E}_{\beta^+}$], 740 keV [89%]) is of major interest because it can be produced from a ^{68}Ge/^{68}Ga generator, making it easily available, inexpensive, and independent of an on-site cyclotron (*10,11*). ^{64}Cu (half-life, 12.7 h; $\bar{E}_{\beta^+}$, 278 keV [17.9%]) is of interest because it can be produced with no carrier added in high quantities with a medical cyclotron via the ^{64}Ni(p,n)^{64}Cu reaction (*12*). In addition, the longer half-life of ^{64}Cu may make it superior to ^{68}Ga if imaging at later time points is needed—important for slowly targeting or clearing radiotracers. We and others found that the chelate moiety coupled to a pharmacophoric peptide may influence the biologic properties of radiopeptides (*13–15*); therefore, we set out to study biologic and pharmacologic properties of somatostatin-based antagonists coupled to different chelating systems.

In the present study, we investigated the influence of the chelator and radiometal on in vitro and in vivo performance of a somatostatin-based antagonist, *p*-Cl-Phe-cyclo(D-Cys-Tyr-D-Aph(Cbm)-Lys-Thr-Cys)D-Tyr-NH_2 (LM3) (D-Aph (Cbm) is D-4-amino-carbamoyl-phenylalanine). As chelators, we chose CB-TE2A because it forms ultrastable copper (II) complexes (*9,16*), and we chose 1,4,7-triazacyclononane,1-glutaric acid, 4,7-acetic acid (NODAGA) because it forms stable complexes with both copper(II) and gallium(III) (*15,17*). NODAGA is an ideal chelator for radiogallium(III) (*17*) and possibly outperforms the commonly used DOTA as a radiogallium chelator. Therefore, we also evaluated DOTA-LM3 labeled with ^{68}Ga.

We studied labeling conditions with ^{64}Cu and ^{68}Ga, binding affinity of the metallopeptides, receptor subtype selectivity, antagonist potency, lipophilicity, pharmacokinetics, and PET images. This study clearly demonstrates that the affinity and pharmacokinetics of the somatostatin-based radioantagonists strongly depend on the chelator and radiometal. In addition, we identified 3 promising PET probes for in vivo imaging of sst2-positive tumors.

MATERIALS AND METHODS

General

All commercial chemicals were of analytic grade. The RinkAmide methylbenzhydrylalanine (MBHA) resin and 9-fluorenylmethoxycarbonyl (Fmoc) amino acids were purchased from NovaBiochem AG and Bachem. $^{64}CuCl_2$ was from University Hospital Tübingen. The ^{68}Ge/^{68}Ga generator was available from Eckert & Ziegler. The reversed-phase high-performance liquid chromatography (RP-HPLC) systems, the γ-counter, and the electrospray ionization mass spectrometer were the same as previously reported (*18*).

Synthesis of Conjugates

The chemical structure of the conjugate NODAGA-LM3 is shown in Figure 1. The Fmoc-D-4-amino-Phe-carbamoyl(tBu)-OH (tBu = *tert*-butyl) was synthesized starting from Fmoc-4-amino-D-Phe(Boc)-OH (Boc = *tert*-butoxycarbonyl), as previously described (*19*). Boc was removed using a 48/48/2/2 mixture of trifluoroacetic acid/dichloromethane/triisopropylsilan/H_2O for 2 h at room temperature (RT). Fmoc-D-4-amino-Phe-OH and 1.5 equivalents of diisopropylethylamine in dry *N,N*-dimethylformamide were stirred with 3 equivalents of *tert*-butyl isocyanate for 3 d. The Fmoc-D-4-amino-Phe-carbamoyl(tBu)-OH was obtained after evaporation and extraction with ethyl acetate/H_2O 3/2.

The peptide–chelator conjugates were synthesized by parallel standard Fmoc solid-phase synthesis on RinkAmide MBHA resin. The Fmoc-protected *p*-Cl-Phe-OH, D-Tyr(tBu)-OH, Cys(Acm)-OH, Thr(tBu)-OH, Lys(Boc)-OH, D-4-amino-Phe-carbamoyl(tBu)-OH, Tyr(tBu)-OH, and D-Cys(Acm)-OH (Acm = acetamidomethyl) were used in a 2-equivalent excess based on the original substitution of the resin. The couplings were mediated by incubating 2 equivalents of 2-(7-Aza-1H-benzotriazole-1-yl)-1,1,3,3-tetramethyluronium hexafluorophosphate in *N,N*-dimethylformamide with 4 equivalents of diisopropylethylamine for 1 h. Fmoc removal was achieved with 20% piperidine in *N,N*-dimethylformamide in two 10-min treatments. Cyclization was performed on the resin with 1.5 equivalents of $Tl(CF_3COO)_3$ at 0°C for 80 min. The prochelators $DOTA(tBu)_3$ and $NODAGA(tBu)_3$ (Chematech) and CB-TE1A1A(tBu) (synthesis will be published elsewhere) were coupled to the N terminus of the peptide by 2-h reaction incubation, using 2-(7-Aza-1H-benzotriazole-1-yl)-1,1,3,3-tetramethyluronium hexafluorophosphate as an activating agent. The conjugates were

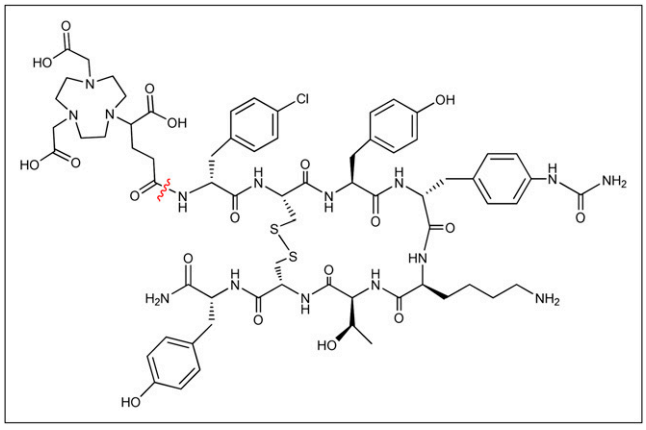

FIGURE 1. Structure of conjugate NODAGA-LM3. In conjugates CB-TE2A-LM3 and DOTA-LM3, chelators CB-TE2A and DOTA, respectively, are coupled to N terminus of LM3 (indicated by red line).

cleaved from the resin and deprotected using 95/2.5/2.5 trifluoroacetic acid/triisopropylsilan/H_2O and precipitated with cold diethyl ether. The final products, CB-TE2A-LM3, NODAGA-LM3, and DOTA-LM3, were purified by semipreparative HPLC and characterized by electrospray ionization mass spectrometry and RP-HPLC.

Preparation of ^{64}Cu and ^{68}Ga Radiopeptides and ^{nat}Cu and ^{nat}Ga Metallopeptides

^{64}Cu-CB-TE2A-LM3 and ^{64}Cu-NODAGA-LM3 were prepared by incubating 5 μg of each conjugate with 37 MBq of $^{64}CuCl_2$ in ammonium acetate (0.1 mol/L, pH 8.0), at 95°C for 30 min (CB-TE2A-LM3) or at RT for 10 min (NODAGA-LM3). ^{68}Ga-NODAGA-LM3 and ^{68}Ga-DOTA-LM3 were prepared in sodium acetate buffer (0.2 mol/L, pH 4.0), at RT for 10 min (NODAGA-LM3) or at 95°C for 8 min (DOTA-LM3), as described elsewhere (*20*). ^{64}Cu and ^{68}Ga radiopeptides were prepared without any postlabeling purification step. Quality control was performed by RP-HPLC.

The ^{nat}Cu and ^{nat}Ga metallopeptides were prepared using a 2-fold excess of $^{nat}CuCl_2 \times 2H_2O$ or $^{nat}Ga(NO_3)_3 \times H_2O$, at the same conditions used for labeling. Free metal ions were removed by SepPak C-18 purification (Waters). The metallopeptides were eluted with ethanol, followed by evaporation to dryness, dissolution in water, and lyophilization.

Determination of Lipophilicity

Each radiopeptide was added to a presaturated 1/1 mixture of phosphate-buffered saline (PBS)/octanol, at a concentration of 15 and 150 pmol/L. The mixtures were vigorously shaken for 1 h and then centrifuged. The activity concentrations of equal volume samples of both phases were measured in a γ-counter, and the partition coefficient (log D) was calculated.

Affinity Determination by Receptor Autoradiography

Receptor autoradiography was performed on 20-μm-thick cryostat sections of membrane pellets prepared from sst1-, sst2-, sst3-, sst4-, and sst5-expressing cells, as previously described (*21,22*). The half maximal inhibitory concentration (IC_{50}) was estimated for each metallopeptide by complete displacement experiments using the universal somatostatin radioligand [Leu^8,D-Trp^{22},^{125}I-Tyr^{25}]-somatostatin-28 (Anawa) and increasing concentrations of the metallopeptide, as previously described (*21,22*).

Immunofluorescence Microscopy–Based Internalization Assay

An immunofluorescence microscopy–based internalization assay was performed on HEK-sst2 cells, provided by Dr. Stefan Schulz, after treatment with the various metallopeptides or [Tyr^3]octreotide (Novartis) using the sst2-specific primary antibody R2-88 (*23*), provided by Dr. Agnes Schonbrunn, as previously described (*24*).

Receptor-Binding, Internalization, and Dissociation Studies

The internalization and dissociation rates of ^{64}Cu-CB-TE2A-LM3 and ^{64}Cu-NODAGA-LM3 were studied in HEK-sst2 cells seeded in 6-well plates, as described previously (*18,20*). Briefly, the radiopeptide was added to the medium (0.25 pmol/mL), and the cells were incubated at 37°C. The internalization was stopped at 0.5, 1, 2, and 4 h by removing the medium and washing the cells with ice-cold PBS. The cells were then treated twice for 5 min with ice-cold glycine solution (0.05 mol/L, pH 2.8), to distinguish between cell surface–bound (acid releasable) and internalized (acid resistant) radiopeptides. Finally, the cells were detached with NaOH (1 mol/L) at 37°C. Internalization was expressed as percentage of the applied radioactivity.

For the dissociation experiments, the plates were placed on ice for 30 min. The radiopeptide was added to the medium (0.25 pmol/mL) and allowed to bind to the cells for 2 h at 4°C. The cells were then quickly washed with ice-cold PBS, and 1 mL of fresh prewarmed (37°C) medium was added. The cells were incubated at 37°C for 10, 20, 30, 60, 120, and 240 min. The medium was collected for quantification, and the cells were treated, as described previously (*18,20*). Nonspecific binding and internalization were determined using a 1,000-fold excess of DOTA-LM3.

In Vivo Biodistribution Studies

Procedures were approved by the authorities in accordance with the Swiss regulations for animal treatment (approval no. 789) and the guidelines of the German Law for the use of living animals in scientific studies. Female athymic nude mice, 4–6 wk old, were injected subcutaneously in the right shoulder with 10^7 HEK-sst2 cells, freshly suspended in 100 μL of sterile PBS. The tumors were allowed to grow for 14–18 d (tumor weight, 100–200 mg).

Mice were injected with a 100 μL/10 pmol/0.15 MBq dose of ^{64}Cu-CB-TE2A-LM3 or ^{64}Cu-NODAGA-LM3 via the tail vein and were euthanized at 1, 4, and 24 h after injection. Mice injected with a 100 μL/10 pmol/0.35 MBq dose of ^{68}Ga-NODAGA-LM3 or ^{68}Ga-DOTA-LM3 were euthanized at 1 h after injection. Nonspecific uptake of all radiopeptides was determined with a coinjection of a 2,000-fold excess of DOTA-LM3. Organs of interest and blood were collected, rinsed of excess blood, blotted dry, weighed, and counted in a γ-counter. The results were expressed as percentage injected dose per gram of tissue (%ID/g) and represent the mean ± SD of $n = 3$–7. The total counts injected per mouse were determined by extrapolation from counts of a known aliquot of the injected solution.

Small-Animal PET Studies

Small-animal PET images were obtained using a dedicated small-animal PET scanner (Focus 120 microPET scanner; Concorde Microsystems Inc.). About 150 pmol/100 μL of each ^{64}Cu- or ^{68}Ga-labeled LM3 (2–3 or 5–6 MBq, respectively) were intravenously injected into the tail vein. Animals were anesthetized with 1.5% isoflurane, and static scans were acquired at 1, 4, and 24 h after injection, for 20 up to 60 min. Blocking experiments were performed, and static scans were obtained at 1 h after injection. PET images were reconstructed with filtered backprojection. No correction was applied for attenuation. Images were generated using AMIDE software (*25*). The color scale was set from 0% to 20% to allow for qualitative comparison among the images.

Data Analysis

Statistical analysis was performed by unpaired 2-tailed t test using Prism software (GraphPad Software Inc.). P values of less than 0.05, less than 0.01, and less than 0.001 were considered significant.

RESULTS

Synthesis of Peptide–Chelator Conjugates and Radiochemistry

NODAGA-LM3, CB-TE2A-LM3, and DOTA-LM3 were obtained with 95% purity or greater, as determined by RP-HPLC, and characterized by electrospray ionization mass spectrometry (Supplemental Table 1 [supplemental materi-

als are available online only at http://jnm.snmjournals.org]; Fig. 1). The labeling with the radiometals was straightforward. NODAGA-LM3 was labeled at RT with ^{64}Cu and ^{68}Ga, in labeling yields greater than 97% and specific activities of 20 and 120 MBq/nmol, respectively. Preparation of ^{64}Cu-CB-TE2A-LM3 in greater than 95% yield was possible after incubation for 30 min at 95°C, at a specific activity of 15 MBq/nmol. ^{68}Ga-DOTA-LM3 was prepared after incubation for 8 min at 95°C, at a specific activity of 100 MBq/nmol.

Binding Affinity and Immunofluorescence Microscopy

All 4 metallopeptides show high selectivity for sst2. IC_{50} values were greater than 10^3 for sst1, sst3, sst4, and sst5. A strong affinity dependence on the attached chelator and also the radiometal was found (Table 1). The IC_{50} values vary 10-fold between $^{68/nat}$Ga-NODAGA-LM3 and $^{68/nat}$Ga-DOTA-LM3, whereas a 1.6-fold difference was found between $^{64/nat}$Cu-NODAGA-LM3 and $^{64/nat}$Cu-CB-TE2A-LM3 and a 5-fold difference between $^{64/nat}$Cu-NODAGA-LM3 and $^{68/nat}$Ga-NODAGA-LM3.

The antagonist properties of the 4 metallopeptides were confirmed by immunofluorescence. Figure 2 illustrates that a 10 nmol/L concentration of the agonist [Tyr^3]octreotide triggers receptor internalization whereas ^{nat}Ga-NODAGA-LM3 at a much higher concentration (1,000 nmol/L) does not stimulate receptor internalization. However, given along with [Tyr^3]octreotide (10 nmol/L), ^{nat}Ga-NODAGA-LM3 and the other metallopeptides are able to efficiently antagonize receptor internalization induced by the agonist. No receptor internalization was seen in the control HEK-sst2 cells treated with vehicle alone (data not shown).

Cell Uptake and Fate of sst2-Bound Radiopeptides

The cell uptake and internalization kinetics of ^{64}Cu-NODAGA-LM3 and ^{64}Cu-CB-TE2A-LM3 were studied in HEK-sst2 cells. Within 30 min approximately 30% of the total added activity is bound to the cell surface for both radiopeptides, and this percentage increased with time up to approximately 40% at 2 h (Supplemental Fig. 2A). The internalized fraction is increasing with time, from 30 min to 4 h, when 12%–13% of the total added activity is internalized (Supplemental Fig. 2B). Nonspecific internalization was less than 1% (data not shown), indicating that the internalization process is specific and receptor-mediated.

The fate of ^{64}Cu-NODAGA-LM3 and ^{64}Cu-CB-TE2A-LM3 bound to the receptor was studied by a temperature-shift experiment. The radiopeptides were allowed to bind at 4°C (to avoid internalization), the temperature was quickly shifted to 37°C, and the concentrations on the cell surface, in the medium and inside the cell, were determined up to 4 h. Figure 3 summarizes the kinetics of the different pathways. The medium is devoid of free radiopeptide at the start of the experiment. ^{64}Cu-NODAGA-LM3 shows a fast disappearance from the receptor, leveling off after 4 h at approximately 55% of radioactivity still receptor-bound. Within 4 h, 16% of the receptor-bound activity is internalized and 26% is released into the medium. ^{64}Cu-CB-TE2A-LM3 (~2-fold-higher receptor affinity) levels off at approximately 70% still bound at 4 h; approximately 15% of sst2-bound radiopeptide is internalized and approximately 15% is dissociated into the medium.

Biodistribution Studies

Table 2 summarizes the biodistribution of ^{64}Cu-NODAGA-LM3 and ^{64}Cu-CB-TE2A-LM3 at 1, 4, and 24 h after injection in HEK-sst2 xenografts. The pharmacokinetics of the radiopeptides are characterized by a fast blood clearance and a high tumor uptake for ^{64}Cu-NODAGA-LM3 and ^{64}Cu-CB-TE2A-LM3 at 1 h (35.46 ± 5.70 %ID/g and 19.26 ± 3.75 %ID/g, respectively, $P < 0.05$) and 4 h (37.88 ± 3.43 %ID/g and 26.87 ± 3.28 %ID/g, respectively, $P < 0.05$). The uptake in the tumor is blocked by an excess of DOTA-LM3 (~98% of ^{64}Cu-NODAGA-LM3 and ~85% of ^{64}Cu-CB-TE2A-LM3) and is also blocked in the sst2-positive organs, such as pancreas and stomach. Less than 50% of ^{64}Cu-NODAGA-LM3 uptake remained in the tumor at 24 h after injection, whereas almost no washout was observed for ^{64}Cu-CB-TE2A-LM3. A significant amount of radioactivity accumulated in the kidneys for both radiopeptides, but accumulation was 2- to 9-fold higher for ^{64}Cu-CB-TE2A-LM3, depending on the time point. The tumor–to–normal-tissue ratios are high for both radiopeptides and increase with time, whereas significantly higher ratios are achieved with ^{64}Cu-NODAGA-LM3 than with ^{64}Cu-CB-TE2A-LM3 (Fig. 4).

^{68}Ga-NODAGA-LM3 and ^{68}Ga-DOTA-LM3 were compared at 1 h after injection. The data are reported in Table 3. Both radiopeptides were concentrated in the tumor (37.27 ± 5.49 %ID/g and 28.72 ± 5.56 %ID/g, respectively), kidneys,

TABLE 1
Characteristics of Metallopeptides

Metallopeptide	IC_{50} (nmol/L)	Peptide charge	Log D
$^{64/nat}$Cu-NODAGA-LM3	6.7 ± 1.5	0	−2.02 ± 0.01
$^{64/nat}$Cu-CB-TE2A-LM3	4.2 ± 1.6	+2	−1.36 ± 0.25
$^{68/nat}$Ga-NODAGA-LM3	1.3 ± 0.3	+1	−2.33 ± 0.22
$^{68/nat}$Ga-DOTA-LM3	12.5 ± 4.3	+1	−2.13 ± 0.01

IC_{50} values are mean ± SEM ($n = 2$) for sst2, and log D values are mean ± SD ($n = 3$).

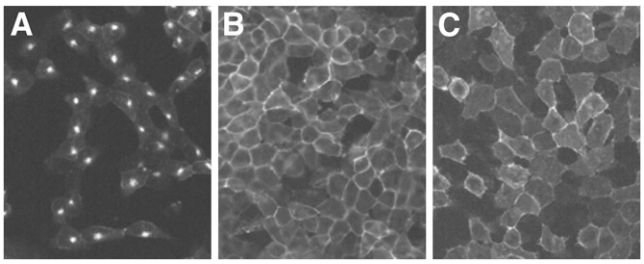

FIGURE 2. sst2 internalization stimulated by [Tyr^3]octreotide is efficiently antagonized by ^{nat}Ga-NODAGA-LM3. HEK-sst2 cells were treated either with [Tyr^3]octreotide (10 nmol/L) (A), a concentration inducing a submaximal sst2 internalization effect, or with ^{nat}Ga-NODAGA-LM3 (1,000 nmol/L) (B). To test for antagonism, HEK-sst2 cells were treated with [Tyr^3]octreotide (10 nM) together with ^{nat}Ga-NODAGA-LM3 (1,000 nmol/L) (C). Although ^{nat}Ga-NODAGA-LM3 at concentration of 1,000 nmol/L is not able to stimulate sst2 internalization, it efficiently antagonizes [Tyr^3]octreotide (10 nmol/L) agonistic effect.

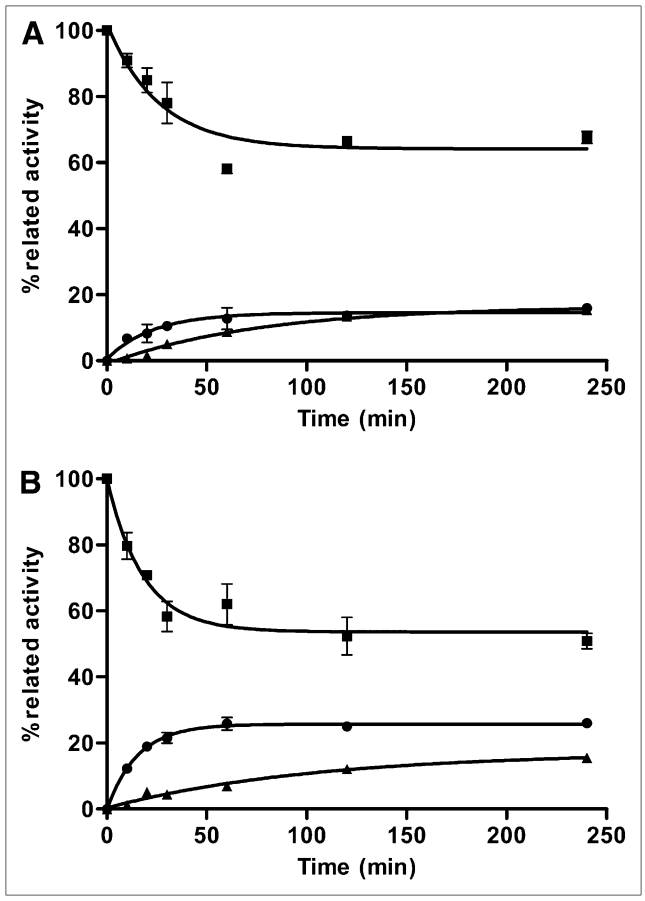

FIGURE 3. Fate of receptor-bound ^{64}Cu-CB-TE2A-LM3 (A) and ^{64}Cu-NODAGA-LM3 (B) in HEK-sst2 after 2 h at 4°C, present as free (●), surface-bound (■), and internalized (▲) radiopeptide, was studied with temperature-shift experiment at 37°C at specified time points. Each time point is average ± SD of triplicate wells corrected for nonspecific binding.

and sst2-positive organs. Again, high tumor uptake, in particular for ^{68}Ga-NODAGA-LM3, was noticeable and comparable to ^{64}Cu-NODAGA-LM3. The tumor–to–normal-tissue ratios were already high at 1 h, when ^{68}Ga-NODAGA-LM3 showed about 2-fold-higher tumor-to-blood and tumor-to-kidney ratios than did ^{68}Ga-DOTA-LM3 (Table 3).

Imaging Studies

Figure 5A shows the small-animal PET images of ^{64}Cu-NODAGA-LM3 and ^{64}Cu-CB-TE2A-LM3 at 4 and 24 h after injection. The images illustrate the high tumor uptake of ^{64}Cu-NODAGA-LM3 and excellent tumor-to-background (in particular tumor-to-kidney) ratio, which is superior to that of ^{64}Cu-CB-TE2A-LM3. Small-animal PET images of ^{68}Ga-NODAGA-LM3 and ^{68}Ga-DOTA-LM3 at 1 h (Fig. 5B) show the high accumulation of the radiopeptides in the tumor and also their specificity (because tumor blocking was demonstrated).

DISCUSSION

Radiolabeled antagonist peptides targeting G-protein–coupled receptor are a new class of tumor targeting vectors. Preclinical (*8*) and preliminary clinical studies (*26*) using somatostatin-based radioantagonists showed surprising results in regard to high tumor uptake and good tumor retention. Relatively little is known in regard to structural parameters determining the pharmacologic properties of somatostatin-based radioantagonists. In the present work, we studied a new somatostatin antagonist, LM3, whose structure is based on known structural motifs leading to somatostatin antagonists (*22*). Three chelators—CB-TE2A, NODAGA, and DOTA—and 2 radiometals—^{64}Cu and ^{68}Ga—were used to study the influence of the chelate on functional parameters and pharmacokinetics of the radiopeptides. The main goal was to develop a PET radiopharmaceutical for clinical application.

^{64}Cu-CB-TE2A-LM3, ^{64}Cu-NODAGA-LM3, ^{68}Ga-NODAGA-LM3, and ^{68}Ga-DOTA-LM3 were prepared in high labeling yields and specific activities, without the need for a postlabeling purification step. All metallopeptides show exclusive sst2 affinity. Affinity, and also pharmacokinetics, strongly depended on the chelate; for example, $^{68/nat}$Ga-NODAGA-LM3 has a 10-fold- and a 5-fold-higher sst2 affinity than $^{68/nat}$Ga-DOTA-LM3 and $^{64/nat}$Cu-NODAGA-LM3, respectively, indicating that there is a much stronger influence of the appended chelate than found in somatostatin-based agonists (*17*). Not enough data are available yet to explain these differences. High-resolution nuclear magnetic resonance data and conformational analysis may possibly help to explain the differences (*27*).

All metallopeptides demonstrated antagonist potency in immunofluorescence microscopy–based internalization experiments; they did not trigger sst2 receptor internalization and antagonized the receptor internalization mediated by an agonist. Interestingly, both ^{64}Cu-NODAGA-LM3 and ^{64}Cu-CB-TE2A-LM3 showed significant levels of internalization in HEK-sst2 cells, although much lower than the internalization of corresponding radioagonists. It is not yet clear why these antagonists internalize in a radiopeptide experi-

TABLE 2
Biodistribution Results of ^{64}Cu-CB-TE2A-LM3 and ^{64}Cu-NODAGA-LM3 in Nude Mice Bearing HEK-sst2 Tumor Xenografts

Organ	1 h	4 h	4 h blocking*	24 h
^{64}Cu-CB-TE2A-LM3				
Blood	0.79 ± 0.32	0.19 ± 0.09	0.12 ± 0.01	0.17 ± 0.08
Heart	0.75 ± 0.15	0.25 ± 0.03	0.12 ± 0.03	0.21 ± 0.07
Liver	5.66 ± 0.67	4.44 ± 1.89	4.35 ± 0.27	3.25 ± 0.70
Spleen	3.16 ± 0.89	1.30 ± 0.27	0.79 ± 0.28	1.04 ± 0.26
Lung	8.27 ± 1.17	4.45 ± 1.17	0.90 ± 0.19	2.46 ± 0.81
Kidney	19.78 ± 3.99	19.57 ± 3.85†	16.40 ± 0.86	11.05 ± 2.81†
Stomach	27.92 ± 3.04	21.79 ± 4.13	0.50 ± 0.12	5.61 ± 1.66
Intestine	3.41 ± 0.59	1.21 ± 0.40	0.33 ± 0.04	0.55 ± 0.13
Adrenal	6.16 ± 1.59	2.38 ± 0.88	0.01 ± 0.01	3.92 ± 1.02
Pancreas	43.89 ± 13.54	20.99 ± 4.80	0.25 ± 0.03	3.37 ± 1.55
Muscle	0.48 ± 0.25	0.23 ± 0.07	0.05 ± 0.01	0.30 ± 0.13
Bone	2.89 ± 1.30	1.57 ± 0.41	0.32 ± 0.11	1.50 ± 0.36
Tumor	19.26 ± 3.75‡	26.87 ± 3.28‡	3.83 ± 1.06	21.55 ± 2.14†
^{64}Cu-NODAGA-LM3				
Blood	0.84 ± 0.10	0.11 ± 0.05	0.10 ± 0.02	0.12 ± 0.05
Heart	0.54 ± 0.08	0.14 ± 0.07	0.20 ± 0.01	0.19 ± 0.08
Liver	2.23 ± 0.48	0.96 ± 0.14	0.90 ± 0.20	0.78 ± 0.15
Spleen	0.94 ± 0.21	0.21 ± 0.10	0.21 ± 0.06	0.19 ± 0.10
Lung	5.89 ± 1.51	0.60 ± 0.17	0.67 ± 0.25	0.54 ± 0.13
Kidney	10.90 ± 1.10	4.41 ± 0.74†	3.52 ± 0.93	1.25 ± 0.47†
Stomach	9.17 ± 2.49	1.31 ± 0.55	0.43 ± 0.14	0.46 ± 0.17
Intestine	1.35 ± 0.12	0.46 ± 0.04	0.46 ± 0.01	0.33 ± 0.06
Adrenal	0.73 ± 0.15	0.02 ± 0.01	0.22 ± 0.05	0.02 ± 0.01
Pancreas	16.26 ± 4.04	0.55 ± 0.10	0.12 ± 0.03	0.23 ± 0.09
Muscle	0.20 ± 0.03	0.03 ± 0.01	0.02 ± 0.01	0.02 ± 0.01
Bone	2.23 ± 1.01	0.39 ± 0.07	0.01 ± 0.01	0.30 ± 0.16
Tumor	35.46 ± 5.70‡	37.88 ± 3.43‡	0.52 ± 0.18	14.79 ± 2.40†

*Coinjection with 2,000-fold excess of DOTA-LM3.
†$P < 0.01$, statistically significant between ^{64}Cu-CB-TE2A-LM3 and ^{64}Cu-NODAGA-LM3.
‡$P < 0.05$, statistically significant between ^{64}Cu-CB-TE2A-LM3 and ^{64}Cu-NODAGA-LM3.
Results are %ID/g ± SD (n = 3–7).

ment (a phenomenon also observed by others (*9*)) but are not able to stimulate sst2 internalization. The explanation might be that ligand trafficking is monitored in the radiopeptide experiment, whereas the sst2 receptor trafficking itself is monitored with immunofluorescence microscopy. Also, the amount of peptide used in the 2 experimental settings is different (0.25 nmol/L and ≤1,000 nmol/L, respectively). First, however, in vivo data indicate that receptor internalization is triggered by agonists but apparently not by antagonists (*28*).

These radioantagonists also differ distinctly in their pharmacokinetic properties. Both ^{64}Cu-labeled peptides show high tumor uptake, increasing between 1 and 4 h. The 1.6-fold-better affinity of ^{64}Cu-CB-TE2A-LM3 is not reflected in a higher tumor uptake. ^{64}Cu-NODAGA-LM3 shows a distinctly higher uptake at 1 and 4 h. The liver uptake and blood concentration are smaller for ^{64}Cu-NODAGA-LM3 at all time points, indicating the high stability of the copper(II)–NODAGA complex in vivo. High liver uptake and slow blood clearance usually are judged as being an indication of free Cu^{2+}, which is being sequestered in the liver, and was typically seen when the ^{64}Cu-DOTA complex was used (*15,16*). The faster background clearance of ^{64}Cu-NODAGA-LM3 may be explained by its higher hydrophilicity and the lower kidney uptake by its neutral charge. The positively charged ^{64}Cu-CB-TE2A-LM3 was expected to have higher kidney uptake due to the negative charge of the renal brush border membrane. Extensive studies on ^{99m}Tc-labeled peptides have clearly shown that decreasing the lipophilicity and the net negative charge of the radiopeptide improves background clearance and increases renal excretion (*13,14*). ^{64}Cu-NODAGA-LM3 shows much higher tumor–to–normal-tissue ratios, an important parameter for good image contrast; this is especially impressive for the tumor-to-kidney ratios, which strongly increase with time and are much higher than usually seen with somatostatin-based radioagonists.

A still unsolved but important general question about tumor targeting is why the radioantagonist shows long retention in the tumor. Our earlier work indicated that low or absent internalization correlates with short tumor retention (*29*). In our present examples, a low internalization was

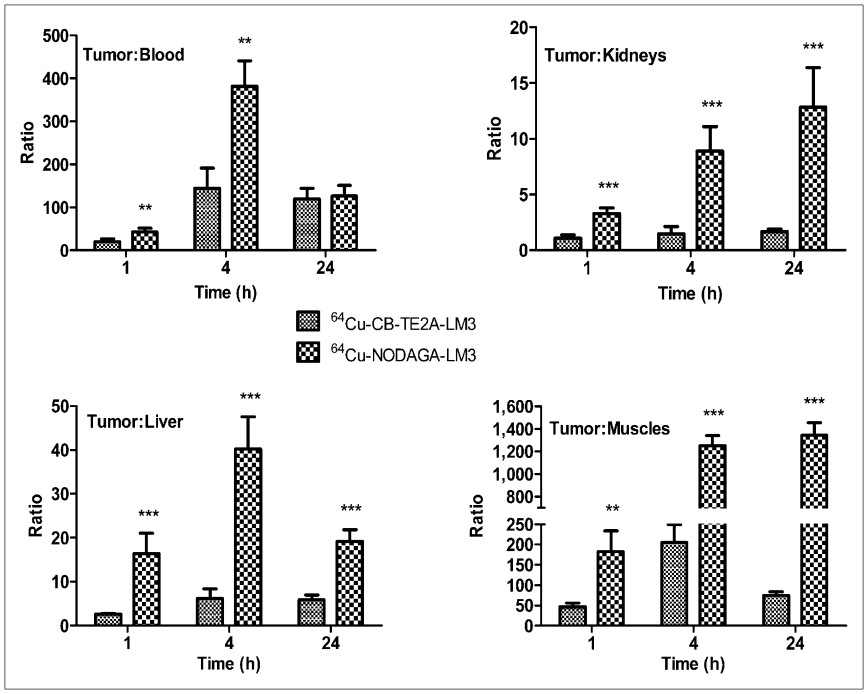

FIGURE 4. Tumor–to–normal-tissue ratios in HEK-sst2 tumor xenografts at 1, 4, and 24 h after injection are significantly higher for ^{64}Cu-NODAGA-LM3 than for ^{64}Cu-CB-TE2A-LM3. $^{**}P < 0.01$. $^{***}P < 0.001$.

found for both ^{64}Cu-labeled peptides. ^{64}Cu-NODAGA-LM3 has a (relatively) slow but distinctly faster washout from the tumor and from sst2-positive organs, such as the pancreas, than does ^{64}Cu-CB-TE2A-LM3. ^{64}Cu-CB-TE2A-LM3 shows almost no washout between 4 and 24 h. This may be of high importance if therapy is considered with the β-emitter ^{67}Cu (half-life, 64 h), because the area under the curve may be larger for the $^{64/67}$Cu-CB-TE2A conjugate. Highly internalizing agonists such as ^{64}Cu-CB-TE2A-TATE show greater than 50% washout between 4 and 24 h (*9*), a value similar to the one we found for the tumor washout of ^{64}Cu-NODAGA-LM3. The explanation for the long retention is not clear yet, and we can only hypothesize. Rebinding of the ligand is a mechanism to explain in vivo long-lasting binding (*30*). High target density, high association rate, and local phenomena, such as chaotic vessels in the tumor, may hinder the diffusion of free radiopeptide molecules from the tumor compartment. We may then explain the fast washout from the pancreas with a more effective perfusion of this organ, a much more organized blood vessel system, and a potentially higher protease activity.

TABLE 3
Biodistribution Results of ^{68}Ga-NODAGA-LM3 and ^{68}Ga-DOTA-LM3 in Nude Mice Bearing HEK-sst2 Tumor Xenografts at 1 Hour After Injection

Organ	^{68}Ga-NODAGA-LM3	^{68}Ga-DOTA-LM3
Blood	0.91 ± 0.01	1.21 ± 0.38
Heart	0.50 ± 0.02	0.42 ± 0.12
Liver	1.08 ± 0.08	0.84 ± 0.20
Spleen	0.84 ± 0.03	0.58 ± 0.20
Lung	3.01 ± 0.54	1.73 ± 0.67
Kidney	19.68 ± 3.30*	32.50 ± 0.66*
Stomach	5.36 ± 1.45	1.08 ± 0.34
Intestine	0.87 ± 0.05	0.56 ± 0.16
Adrenal	2.55 ± 0.31	1.06 ± 0.64
Pancreas	9.15 ± 1.03	0.91 ± 0.22
Muscle	0.36 ± 0.02	0.32 ± 0.03
Bone	2.31 ± 0.66	1.63 ± 0.03
Tumor	37.27 ± 5.49	28.72 ± 5.56
Tumor–to–normal-tissue ratio		
Tumor to blood	41.1 ± 6.2	24.2 ± 3.0
Tumor to liver	34.7 ± 7.5	34.3 ± 1.6
Tumor to kidney	1.9 ± 0.6	0.9 ± 0.2
Tumor to muscle	104.8 ± 22.1	90.6 ± 10.3

*$P < 0.05$, statistically significant.
Results are %ID/g ± SD ($n = 3$).

Perhaps a rebinding mechanism causing the long tumor retention of ^{64}Cu-CB-TE2A-LM3 is somehow reflected in the rate of disappearance of the radiopeptide from the cell surface in vitro. A difference between ^{64}Cu-CB-TE2A-LM3 and ^{64}Cu-NODAGA-LM3 was indeed found when we studied the fate of the receptor-bound radiopeptide. A plateau is already reached for the former at approximately 70% of receptor-bound ^{64}Cu-CB-TE2A-LM3, distinctly higher than with ^{64}Cu-NODAGA-LM3, which levels off only at approximately 55%. It is not clear yet whether the rebinding mechanism is an indication that ^{64}Cu-CB-TE2A-LM3 has insurmountable properties and needs further studies. Interestingly, the internalization kinetics experiments demonstrate slow, almost linear, internalization with time, whereas when the fate of receptor-bound radiopeptide is studied, the internalization kinetics already shows a plateau after about 1 h. This may be explained by 2 different binding sites—one coupling to G proteins and the other to β-arrestin, finally leading to internalization (*31*).

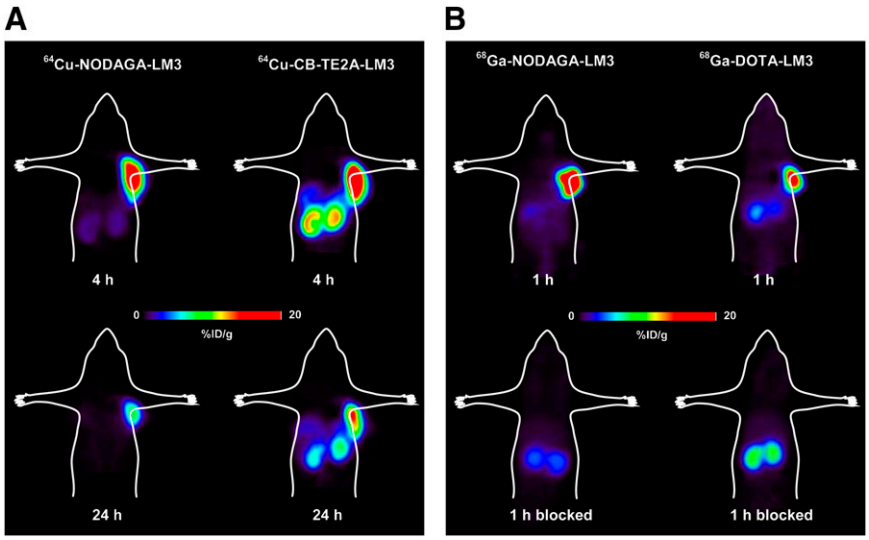

FIGURE 5. (A) Small-animal PET images of ^{64}Cu-NODAGA-LM3 and ^{64}Cu-CB-TE2A-LM3 at 4 and 24 h after injection (coronal sections) show potential of these radiopeptides for in vivo imaging of sst2-expressing tumors and confirm improved tumor-to-background contrast of ^{64}Cu-NODAGA-LM3, especially tumor-to-kidney. (B) Small-animal PET images of ^{68}Ga-NODAGA-LM3 and ^{68}Ga-DOTA-LM3 (coronal sections) show good image contrast at early time points of investigation (1 h after injection) and prove specificity of radiopeptides for sst2 receptors, because no tumor is visualized after coinjection of excess of unlabeled peptide.

A comparison between ^{68}Ga- and ^{64}Cu-labeled peptides is of interest because ^{68}Ga radiopharmacy is reminiscent of kit-based ^{99m}Tc radiopharmacy. ^{68}Ga-NODAGA-LM3 shows the highest tumor uptake at 1 h. ^{68}Ga-NODAGA-LM3 uptake was also higher than ^{68}Ga-DOTA-LM3 uptake in the sst2-positive organs, such as the pancreas. ^{68}Ga-DOTA-LM3 uptake was much lower, reflecting its lower sst2 affinity. The tumor–to–normal-tissue ratios, in particular the tumor-to-blood and tumor-to-muscle ratios, are already high enough for good image quality at this early time point. Small animal PET shows the good contrast already at 1 h, and the blocking study demonstrates the high specificity of the tumor uptake. ^{68}Ga-DOTA-LM3 also shows good pharmacokinetics but is inferior to ^{68}Ga-NODAGA-LM3, considering the tumor and kidney uptake.

When all 4 radiopeptides are compared, ^{64}Cu may have a potential advantage over ^{68}Ga because of the longer half-life. The tumor–to–normal-tissue ratios of the ^{64}Cu-labeled peptides increase with time—an advantage that can be exploited only with a radionuclide with a longer half-life. In the present case, ^{68}Ga may be preferred for the reasons presented here in our current study and considering the much lower radiation burden to the patient.

CONCLUSION

For in vivo imaging of sst2-positive tumors, we have developed 4 PET radiopharmaceuticals showing promising pharmacokinetic properties and a clear potential for translation into the clinic. These radiopharmaceuticals show the high potential of antagonists and may be superior to corresponding agonists. An important and also surprising result of the pharmacokinetic studies is that the chelator makes the difference in regard to tumor uptake and retention, whereas the antagonist LM3 is sensitive to N-terminal modification, a result that was not found to the same extent with octapeptide-based agonists of the octreotide type.

DISCLOSURE STATEMENT

The costs of publication of this article were defrayed in part by the payment of page charges. Therefore, and solely to indicate this fact, this article is hereby marked "advertisement" in accordance with 18 USC section 1734.

ACKNOWLEDGMENTS

We thank Dr. Stephan Schulz for the HEK-sst2–transfected cells, Dr. Rebecca A. Dumont and Friederike Deininger for their support on animal experiments, and Novartis Pharma for analytic assistance. This study was supported in part by the European Commission Research FP7 project TARCC, the COST actions D38 and BM0607, and the Swiss National Science Foundation (no. 320000-118333). No other potential conflict of interest relevant to this article was reported.

REFERENCES

1. Reubi JC, Waser B, Schaer JC, Laissue JA. Somatostatin receptor sst1-sst5 expression in normal and neoplastic human tissues using receptor autoradiography with subtype-selective ligands. *Eur J Nucl Med.* 2001;28:836–846.
2. Kwekkeboom DJ, Kam BL, van Essen M, et al. Somatostatin-receptor-based imaging and therapy of gastroenteropancreatic neuroendocrine tumors. *Endocr Relat Cancer.* 2010;17:R53–R73.
3. Ambrosini V, Campana D, Bodei L, et al. ^{68}Ga-DOTANOC PET/CT clinical impact in patients with neuroendocrine tumors. *J Nucl Med.* 2010;51:669–673.
4. Srirajaskanthan R, Kayani I, Quigley AM, Soh J, Caplin ME, Bomanji J. The role of ^{68}Ga-DOTATATE PET in patients with neuroendocrine tumors and negative or equivocal findings on ^{111}In-DTPA-octreotide scintigraphy. *J Nucl Med.* 2010;51:875–882.
5. Gabriel M, Oberauer A, Dobrozemsky G, et al. ^{68}Ga-DOTA-Tyr3-octreotide PET for assessing response to somatostatin-receptor-mediated radionuclide therapy. *J Nucl Med.* 2009;50:1427–1434.
6. Kwekkeboom DJ, de Herder WW, Kam BL, et al. Treatment with the radiolabeled somatostatin analog [177 Lu-DOTA 0,Tyr3]octreotate: toxicity, efficacy, and survival. *J Clin Oncol.* 2008;26:2124–2130.
7. Bushnell DL Jr, O'Dorisio TM, O'Dorisio MS, et al. ^{90}Y-edotreotide for metastatic carcinoid refractory to octreotide. *J Clin Oncol.* 2010;28:1652–1659.
8. Ginj M, Zhang H, Waser B, et al. Radiolabeled somatostatin receptor antagonists are preferable to agonists for in vivo peptide receptor targeting of tumors. *Proc Natl Acad Sci USA.* 2006;103:16436–16441.
9. Wadas TJ, Eiblmaier M, Zheleznyak A, et al. Preparation and biological evaluation of ^{64}Cu-CB-TE2A-sst2-ANT, a somatostatin antagonist for PET imaging of somatostatin receptor-positive tumors. *J Nucl Med.* 2008;49:1819–1827.

10. Fani M, Andre JP, Maecke HR. ^{68}Ga-PET: a powerful generator-based alternative to cyclotron-based PET radiopharmaceuticals. *Contrast Media Mol Imaging.* 2008;3:67–77.
11. Roesch F, Riss PJ. The renaissance of the ^{68}Ge/^{68}Ga radionuclide generator initiates new developments in ^{68}Ga radiopharmaceutical chemistry. *Curr Top Med Chem.* 2010;10:1633–1668.
12. Obata A, Kasamatsu S, McCarthy DW, et al. Production of therapeutic quantities of ^{64}Cu using a 12 MeV cyclotron. *Nucl Med Biol.* 2003;30:535–539.
13. Decristoforo C, Mather SJ. The influence of chelator on the pharmacokinetics of ^{99m}Tc-labelled peptides. *Q J Nucl Med.* 2002;46:195–205.
14. Rusckowski M, Qu T, Gupta S, Ley A, Hnatowich DJ. A comparison in monkeys of ^{99m}Tc labeled to a peptide by 4 methods. *J Nucl Med.* 2001;42:1870–1877.
15. Prasanphanich AF, Nanda PK, Rold TL, et al. [^{64}Cu-NOTA-8-Aoc-BBN(7-14)NH2] targeting vector for positron-emission tomography imaging of gastrin-releasing peptide receptor-expressing tissues. *Proc Natl Acad Sci USA.* 2007;104:12462–12467.
16. Wadas TJ, Wong EH, Weisman GR, Anderson CJ. Copper chelation chemistry and its role in copper radiopharmaceuticals. *Curr Pharm Des.* 2007;13:3–16.
17. Eisenwiener KP, Prata MI, Buschmann I, et al. NODAGATOC, a new chelator-coupled somatostatin analogue labeled with [67/^{68}Ga] and [^{111}In] for SPECT, PET, and targeted therapeutic applications of somatostatin receptor (hsst2) expressing tumors. *Bioconjug Chem.* 2002;13:530–541.
18. Antunes P, Ginj M, Zhang H, et al. Are radiogallium-labelled DOTA-conjugated somatostatin analogues superior to those labelled with other radiometals? *Eur J Nucl Med Mol Imaging.* 2007;34:982–993.
19. Jiang G, Stalewski J, Galyean R, et al. GnRH antagonists: a new generation of long acting analogues incorporating p-ureido-phenylalanines at positions 5 and 6. *J Med Chem.* 2001;44:453–467.
20. Fani M, Mueller A, Tamma ML, et al. Radiolabeled bicyclic somatostatin-based analogs: a novel class of potential radiotracers for SPECT/PET of neuroendocrine tumors. *J Nucl Med.* 2010;51:1771–1779.
21. Reubi JC, Schar JC, Waser B, et al. Affinity profiles for human somatostatin receptor subtypes SST1-SST5 of somatostatin radiotracers selected for scintigraphic and radiotherapeutic use. *Eur J Nucl Med.* 2000;27:273–282.
22. Cescato R, Erchegyi J, Waser B, et al. Design and in vitro characterization of highly sst2-selective somatostatin antagonists suitable for radiotargeting. *J Med Chem.* 2008;51:4030–4037.
23. Gu YZ, Schonbrunn A. Coupling specificity between somatostatin receptor sst2A and G proteins: isolation of the receptor-G protein complex with a receptor antibody. *Mol Endocrinol.* 1997;11:527–537.
24. Cescato R, Schulz S, Waser B, et al. Internalization of sst2, sst3, and sst5 receptors: effects of somatostatin agonists and antagonists. *J Nucl Med.* 2006; 47:502–511.
25. Loening AM, Gambhir SS. AMIDE: a free software tool for multimodality medical image analysis. *Mol Imaging.* 2003;2:131–137.
26. Wild D, Fani M, Behe M, et al. First clinical evaluation of somatostatin receptor antagonist imaging. *J Nucl Med.* 2010;51(suppl 2):134P.
27. Deshmukh MV, Voll G, Kuhlewein A, et al. NMR studies reveal structural differences between the gallium and yttrium complexes of DOTA-D-Phe1-Tyr3-octreotide. *J Med Chem.* 2005;48:1506–1514.
28. Waser B, Tamma ML, Cescato R, Maecke HR, Reubi JC. Highly efficient in vivo agonist-induced internalization of sst2 receptors in somatostatin target tissues. *J Nucl Med.* 2009;50:936–941.
29. Ginj M, Zhang H, Eisenwiener KP, et al. New pansomatostatin ligands and their chelated versions: affinity profile, agonist activity, internalization, and tumor targeting. *Clin Cancer Res.* 2008;14:2019–2027.
30. Vauquelin G, Charlton SJ. Long-lasting target binding and rebinding as mechanisms to prolong in vivo drug action. *Br J Pharmacol.* 2010;161:488–508.
31. Kenakin T, Miller LJ. Seven transmembrane receptors as shapeshifting proteins: the impact of allosteric modulation and functional selectivity on new drug discovery. *Pharmacol Rev.* 2010;62:265–304.